ACS Photonics

pubs.acs.org/journal/apchd5

Perspective

Machine Learning for Integrated Quantum Photonics

Zhaxylyk A. Kudyshev, Vladimir M. Shalaev, and Alexandra Boltasseva*

Cite This: https://dx.doi.org/10.1021/acsphotonics.0c00960

Read Online

ACCESS | Metrics & More | Article Recommendations

ABSTRACT: Realization of integrated quantum photonics is a key step toward scalable quantum applications such as quantum computing, sensing, information processing, and quantum material metrology. To enable practical quantum photonic systems, several challenges should be addressed, including (i) the realization of deterministic, bright, and stable single-photon emission operating at THz rates and at room temperatures, (ii) on-chip integration of efficient single-photon sources, and (iii) the development of deterministic and scalable nanoassembly of quantum circuitry elements. In this Perspective, we focus on the emerging field of physics-informed machine learning (ML) quantum photonics that is envisioned to play a decisive role in addressing the above challenges. Specifically, three directions of ML-assisted quantum research are discussed: (i) rapid preselection of single single-photon sources via ML-assisted quantum measurements, (ii) hybrid ML-optimization approach for developing efficient quantum circuits elements, and (iii) ML-based frameworks for developing novel deterministic assembly of on-chip quantum emitters.

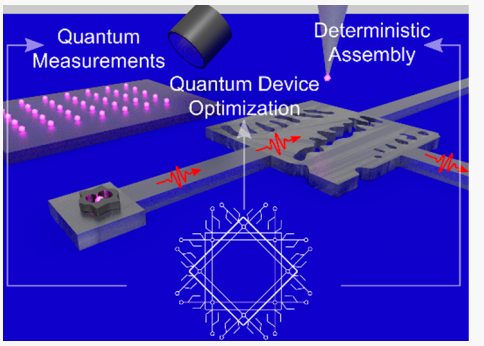

KEYWORDS: *quantum photonics, machine learning, deep neural networks, on-chip quantum optics*

By utilizing quantum entanglement, a tremendous increase in computational efficiency compared to any classical algorithm can be achieved for problems like number factorization (exponential speedup), most optimization, and inverse design problems (quadratic speedup).[1,2] While many physical realizations of qubits have been proposed, including trapped ions and atoms,[3,4] superconducting circuits,[5] quantum dots,[6] solid-state color centers,[7] and photons,[8] the latter offer some unique features. Photons interact very weakly with transparent optical media and not at all among themselves, which renders the information they carry robust against decoherence. However, the photons' relatively weak interaction with matter brings about two major issues in photonic quantum technologies. First, nondeterministic logical operations with photons using linear optical quantum gates put enormous overheads on the required infrastructure and severely limit the operation bandwidth of photonic quantum information processing systems, especially when the gate success rates are low. Second, single photon sources proposed so far, which utilize both quantum emitters and nonlinear media, have not yet provided fast and deterministic streams of indistinguishable photons at room temperature. The single-photon rates in quantum emitters are limited by the spontaneous emission lifetime, while the nonlinear sources fail to produce the single-photons deterministically. Addressing these issues is even more challenging when multiphoton states are required. First, the nondeterministic or slow single-photon emission limits the speed with which such states can be prepared. Second, the time required for quantum correlation measurements and, in particular, the multiphoton quantum state tomography scale very unfavorably with the complexity of the photon state. There is a clear demand for single-photon emitters (SPEs) capable of producing indistinguishable photons and entangled photon states at room temperature and at high emission rates. Most importantly, large-scale quantum circuitry integration and prototyping requires (i) novel rapid characterization techniques for the selection of suitable quantum emitters out of large numbers of potential candidates and (ii) efficient integration of the SPEs into an on-chip environment.

Machine learning (ML) algorithms have already shown great potential for addressing the main bottlenecks in computer vision,[9] natural language processing,[10] speech recognition,[11] and other tasks across materials science,[12] chemistry,[13] laser physics,[14] and microscopy.[15] Recently, ML techniques have been used for the fine-tuning parameters of the semiconductor quantum devices,[16,17] as well as quantum measurement optimization.[18] Similarly, applying advanced ML algorithms to conventional methods in quantum photonics could address the fundamental limitations such as long characterization/read-out times, inefficient assembly, and quantum emitter perform-

Special Issue: 20 Years of Photonics

Received: June 16, 2020
Revised: December 10, 2020
Accepted: December 14, 2020

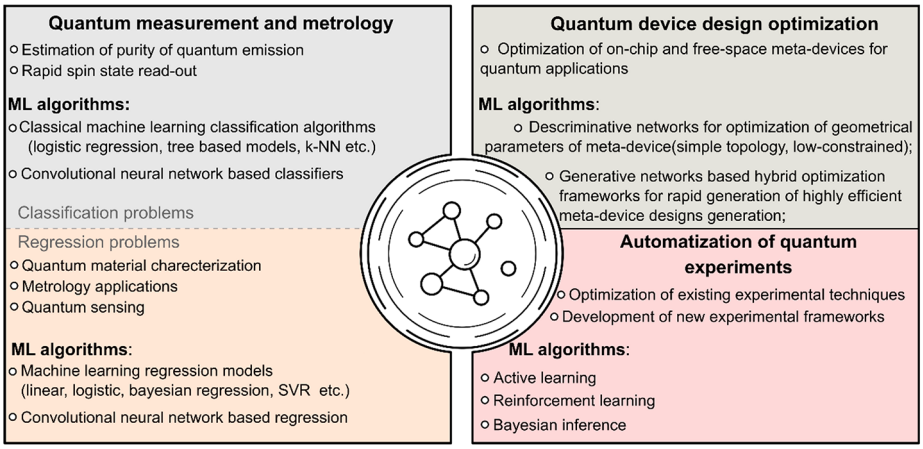

Figure 1. Application of ML techniques in quantum photonics. Different quantum measurements and metrology tasks can be formulated as classification or regression problems. Based on the nature of the problem and available data set properties, different ML- and CNN-based classification/regression models can be applied. The choice of the model is dictated by the nature of the problem and required accuracy. Yet another direction where ML techniques can be used is optimization of on-chip and free-space meta-devices for quantum photonic applications. The discriminative CNNs and generative networks can be adapted for advanced multiparametric and shape/topology optimization of the meta-device designs. Active, reinforcement learning, as well as Bayesian inference algorithms, has been shown to be a promising route for automatization of quantum experiments. Such an approach can be used for the optimization of existing experimental techniques and the development of novel approaches.

ance, as well as help to unlock new physics and application spaces. There are different venues within quantum photonics, where ML techniques have great potential. Figure 1 highlights some of the potential applications with example problems and corresponding ML algorithms. In this Perspective, we highlight some of the key directions of the emerging field of ML assisted quantum photonics. Specifically, we will cover (i) ML techniques for quantum characterization and metrology applications, (ii) ML-assisted quantum photonic device design development, and (iii) active and reinforcement learning for novel quantum experiment development.

QUANTUM MEASUREMENT AND METROLOGY

Due to the statistical complexity of the signal, quantum optical measurements require a long collection time in order to acquire complete data and to retrieve accurate results. Conventionally, statistical methods of data postprocessing play an important role in the interpretation of the results of quantum measurements. The statistical methods have a long-standing focus on inference via creation and fitting problem-specific probability models. Such approaches allow for computing a quantitative measure of confidence of the developed mathematical model based on the acquired noisy data. In contrast, ML frameworks aim at predicting the outcome of the experiment by using general-purpose learning algorithms, which allows one to find correlations between the features of the data sets and the results of the measurement. Such data-driven formalism makes ML frameworks applicable to the quantum photonics problems, where conventional statistical methods fail due to the sparsity of the collected data. This makes ML techniques a unique enabler for the realization of the next-generation, rapid, precise, quantum measurement techniques.

Several quantum material characterization problems can be formulated as a binary or multiclass classification, which should yield a prediction of the predefined categorical variable of the quantum measurement based on the acquired sparse data sets. For example, an estimation of the quantum purity of a quantum emission can be formulated as a binary classification problem within which the class of the emitter ("good"/"bad") is determined based on the sparse autocorrelation measurement. Yet, another example is a spin-state read-out of nitrogen-vacancy centers (NVs) in nanodiamonds, which can be formulated as a binary classification ($|0\rangle$ and $|1\rangle$ spin states) with the goal of minimizing the number of performed read-out cycles. Such problems can be addressed either by classical machine learning algorithms (logistics regression, tree-based models, k-nearest neighbors (kNN),[19] random forest,[20] support vector machine (SVM)[21]) or via convolutional neural network (CNN)-based classifiers. Along with classification problems, quantum measurement and metrology applications can be formulated as a regression, which targets retrieving the exact value of the measurement based on the available sparse information. The ML regression models can be used to retrieve the measured property of the quantum system to reduce the measurement time and to maintain the same level of precision. Such a class of problems can be addressed via various ML-based regression algorithms (linear,[22] logistic,[23] Bayesian regression models[24] support vector machine regression[21]) or CNN-based regression models. The choice of the most suitable ML algorithm for different problems depends on many factors, such as the physics involved, final measurement value/outcome, type of available data sets (complexity, variance, and size), and available computational resources. The common requirement for most of the ML techniques is to gather a sufficient amount of data to get reliable predictions. However, for quantum measurements, this may be excessively time-consuming, which leads to the constraints of the acquired data set, such as reduced variance and the number of the available training sets. Thus, if the size of the training set is small or has a low variance, the algorithms with low variance, for example, linear regression, Naïve Bayes, or SVM can work best for such problems. If the training set is sufficiently large and with a high number of observations in comparison with the number of features, algorithms with high variance (k-NN, tree-based models) might be the best choice. Along with ML

https://dx.doi.org/10.1021/acsphotonics.0c00960
ACS Photonics XXXX, XXX, XXX−XXX

algorithms, the CNN based classification/regression can be adapted for both aforementioned cases. Such versatility of the CNN models is assured by the high flexibility of its structure, which can be adapted for different complexities and variances of the data set.

Another important aspect of the method preference is the accuracy of the model and computational resources required for the training process. Depending on the problem under consideration, different levels of accuracy of the model might be acceptable. In the cases when the accuracy requirement is not so high, it is possible to significantly reduce the computation time by choosing the less accurate model. A qualitative comparison between different ML models applicable for quantum measurements and metrology applications is shown in Figure 2. In most cases, the accuracy and training

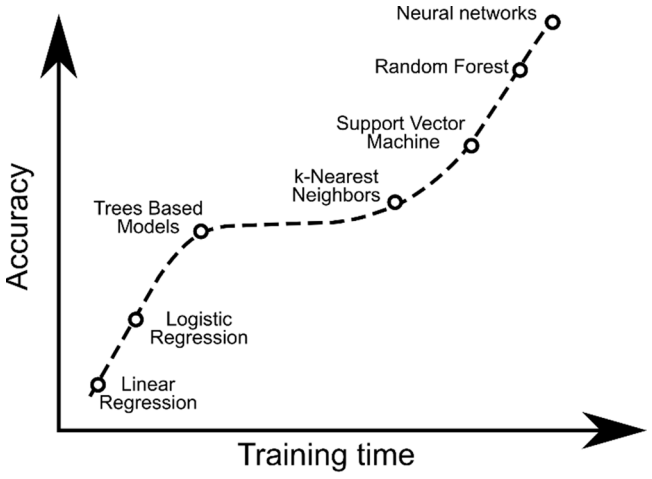

Figure 2. ML model accuracy (fidelity) as a function of required training time. The choice of the model applicable for quantum measurement and metrology application is partially dictated by the required accuracy of the model. Depending on the model complexity different ML models and neural networks ensures different accuracy levels and require different model training time.

speed stand on opposite sides; it is necessary to consider trade-offs between the two when deciding on the choice of the algorithm. The algorithms such as linear/logistic regression and Naïve Bayes are less resource-heavy (easier to train and have fast execution), while the models with high degrees of freedom (SVM, CNN, random forest) ensure higher accuracy, but demand much longer time to process and train.

Recently, various ML algorithms have been adapted for quantum optical measurements and metrology problems.[25−30] It has been demonstrated that a combination of the Bayesian and Hamiltonian learning techniques allows the realization of magnetic field sensing with extreme sensitivity at room temperature using nitrogen-vacancy (NV) centers in bulk diamond[31] (Figure 3a,b). Specifically, Bayesian-learning-assisted spin readout can be used for processing a noisy signal of a single NV center at room temperature and requires on average only one photon per iteration to detect the magnetic field. The developed approach ensures sensitivity values of 60 $nTs^{1/2}$, including initialization, readout, and computational overheads that are comparable to those reported for cryogenic experiments. Additionally, it has been shown that dephasing times can be simultaneously estimated and that time-dependent fields can be dynamically tracked at room temperature. The Hamiltonian learning technique has also been applied for the characterization of electron spin states of NV centers in diamond.[32] In addition, ML algorithms have been used for the development of autonomous adaptive feedback schemes for the quantum measurements.[33,34]

ML algorithms have recently been applied to address the issue of reconstruction of quantum states via quantum tomography[29] (Figure 3c,d) where a deep neural network (DNN) was used to filter noisy experimental data and reconstruct the original states. Particularly, DNNs can address the state-preparation-and-measurement mitigation (SPAM) problem and enhance the fidelity of quantum state reconstruction by 10% and 27% in comparison with a protocol that treats the SPAM errors by process tomography and a SPAM-agnostic protocol, respectively.

The classification of classical and quantum emitters utilizing ML techniques has also attracted significant attention. For example, the adaptive linear element (ADALINE) model was used for the classification of thermal light from coherent light at the single-photon level (Figure 3e,f).[30] The proposed Bayes classifier reduces the number of measurement runs by several orders of magnitude in comparison with conventional schemes.

ML algorithms can also dramatically speed up the characterization of quantum defects and quantum emission and rapidly classify the quality of the emitters as either "good" or "bad".[35] They can also determine the exact value of the quantum emitter specs based on sparse measurements, which require substantially less integration time (Figure 3g). ML methods could potentially transform the area of quantum materials metrology where measuring impurities in high-purity quantum materials has remained a daunting task that requires complex techniques. Certain types of fluorescent defects can be detected using photon autocorrelation experiments. This technique estimates the number of defects in the focus volume of the collection optics by assessing the value of the so-called autocorrelation at zero delay, $g^{(2)}(0)$. This quantity is obtained by fitting an autocorrelation histogram, which represents the number of coincidental detection events on two separate detectors as a function of the delay between the detection times. A scanning autocorrelation procedure provides a local defect density map with the precision down to a single fluorescent object, well above the resolution of the optical setup. However, for small defect concentrations that are typical for quantum materials, the data collection is very slow (tens of minutes) as the speed is proportional to the square of the emission intensity, which is very weak. Recently, it has been demonstrated that supervised ML, as well as DNNs, can be applied to the rapid characterization of quantum emission[35] (Figure 3h). Specifically, both the ML models have been trained to predict the quantum emission purity based on the sparse 1 s autocorrelation measurement. The conventional method (Levenberg−Marquardt fitting) requires a complete data set collected within tens of minutes. The proposed approach allows determining the class of the NV center in a nanodiamond ("single"/"not-single") with more than 95% accuracy and a 100× speed-up of the measurement time. Moreover, the classification criteria between "single" and "not-single" classes can be adjusted without losing any accuracy.

The developed approach can be directly extended to other types of quantum optical measurements that require multiclass classification, thus addressing the problem of long collection time due to the extremely low codetection event probability. By reshaping the binary classification scheme into the

https://dx.doi.org/10.1021/acsphotonics.0c00960
ACS Photonics XXXX, XXX, XXX−XXX

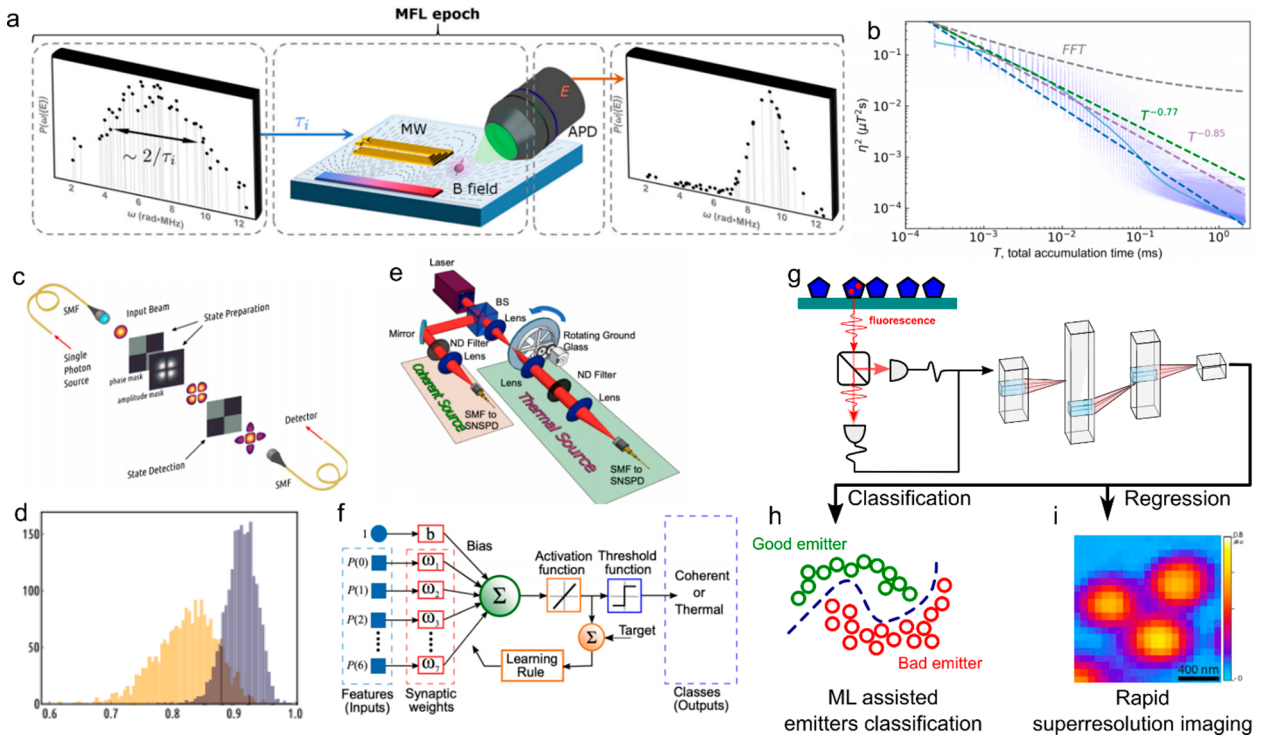

Figure 3. (a, b) ML-assisted magnetic field sensing.[31] (a) Three-step Bayesian inference based magnetic field learning algorithm: (left) the phase accumulation time τ_i of the current iteration is determined based on the electric field measurement done during the previous iteration; (center) measurement of the electric field; (right) measured electric field is used to update the prior distribution using Bayesian inference and determine the phase accumulation time τ_{i+1} for the next iteration. (b) The scaling of the magnetic field sensing precision as a function of the total measurement time. The density plot and blue dashed line show the precision data of the ML-assisted approach and corresponding fitting. For the comparison, the scaling of the precision of conventionally used Fast Fourier Transform (FFT) protocol is shown with gray dashed curve. (c, d) ML-assisted quantum tomography.[29] (c) Experimental setup for preparation and measurement of spatial qudit states. In the generation part, single photons from a heralded source are beam-shaped by a single mode fiber and then transformed by a hologram displayed on a spatial light modulator. Analogously, the detection part consists of a hologram corresponding to the chosen detection mode, followed by a single mode fiber and a single photon counter. (d) Results of the experimental state reconstruction with phase-only holograms. State reconstruction uses maximum likelihood estimation for both raw experimental data (orange) and DNN processed data (blue). (e, f) Coherent vs thermal light classification.[30] (e) In the experiment, a laser beam is divided by a beam splitter (BS) and the two replicas of the beam are used to generate light with Poissonian (coherent) and super-Poissonian (thermal) statistics. The thermal beam is generated by a rotating ground glass. Neutral density (ND) filters are utilized to attenuate light to the single-photon level. Coherent and thermal light beams are measured by superconducting nanowire single-photon detectors (SNSPDs). (f) Flow diagram of the ADALINE neuron used for demonstration of light source identification. (g–i) ML-assisted autocorrelation function measurement. (g) The florescence from an NV center in an nanodimond is passed through the beam splitter and coupled to the correlation card (start–stop scheme). The 1 s autocorrelation histograms are passed through CNN for (h) classification of the quantum emitters ("good"/"bad") or (i) prediction of the exact value of the $g^2(0)$ (regression). (i) The regression scheme can be directly used for rapid super-resolution imaging utilizing autocorrelation $g^2(0)$ map.[36] (a, b) Adapted with permission from ref 31. Copyright 2019 American Physical Society. (c, d) Adapted with permission from ref 29. Copyright 2020 Nature Research. (e, f) Adapted with permission from ref 30. Copyright 2020 American Institute of Physics. (i) Adapted with permission from ref 36. Copyright 2014 American Physical Society.

regression model, it should be possible to predict the exact values of the autocorrelation function at zeroth time delays. This could be used for the realization of rapid super-resolution microscopy based on autocorrelation measurements[36,37] (Figure 3i). Recently, different variations of super-resolution techniques based on the photon antibunching effect have been developed.[36−38] It has been shown that the resolution of such methods scales as $1/\sqrt{n}$, where n is the order of the autocorrelation function of the photoluminescence signal. These techniques have thus far been limited by long image acquisition times.

ML techniques could also be adapted for rapid measurements of other properties of single-photon emitters. One direction could be the realization of RT single-shot spin readout of solid-state quantum defects. Due to the small magnetic moments of the spin states, it remains challenging to realize single-shot readout of individual nuclear spins with high fidelity at ambient environment. The aforementioned supervised ML algorithms can be applied for the classification of different spin states based on the sparse single-shot measurement data.

QUANTUM META-DEVICE DESIGN OPTIMIZATION

Yet another important application of the ML algorithms in quantum optics is a ML-assisted optimization of the on-chip and free-space meta-structures for quantum applications. Recent progress in the fields of material platforms and nanofabrication techniques has led to dramatic progress in communication, computing, biosensing, a field of renewable energy, and quantum information technologies. Specifically, artificially engineered materials, like photonic crystals,[39] metamaterials,[40] and metasurfaces[41,42] have been reviled as a promising route for achieving unparalleled control over the nm-scale light–matter interaction, which led to the realization of a wide range of conceptually new applications. Recently

https://dx.doi.org/10.1021/acsphotonics.0c00960
ACS Photonics XXXX, XXX, XXX−XXX

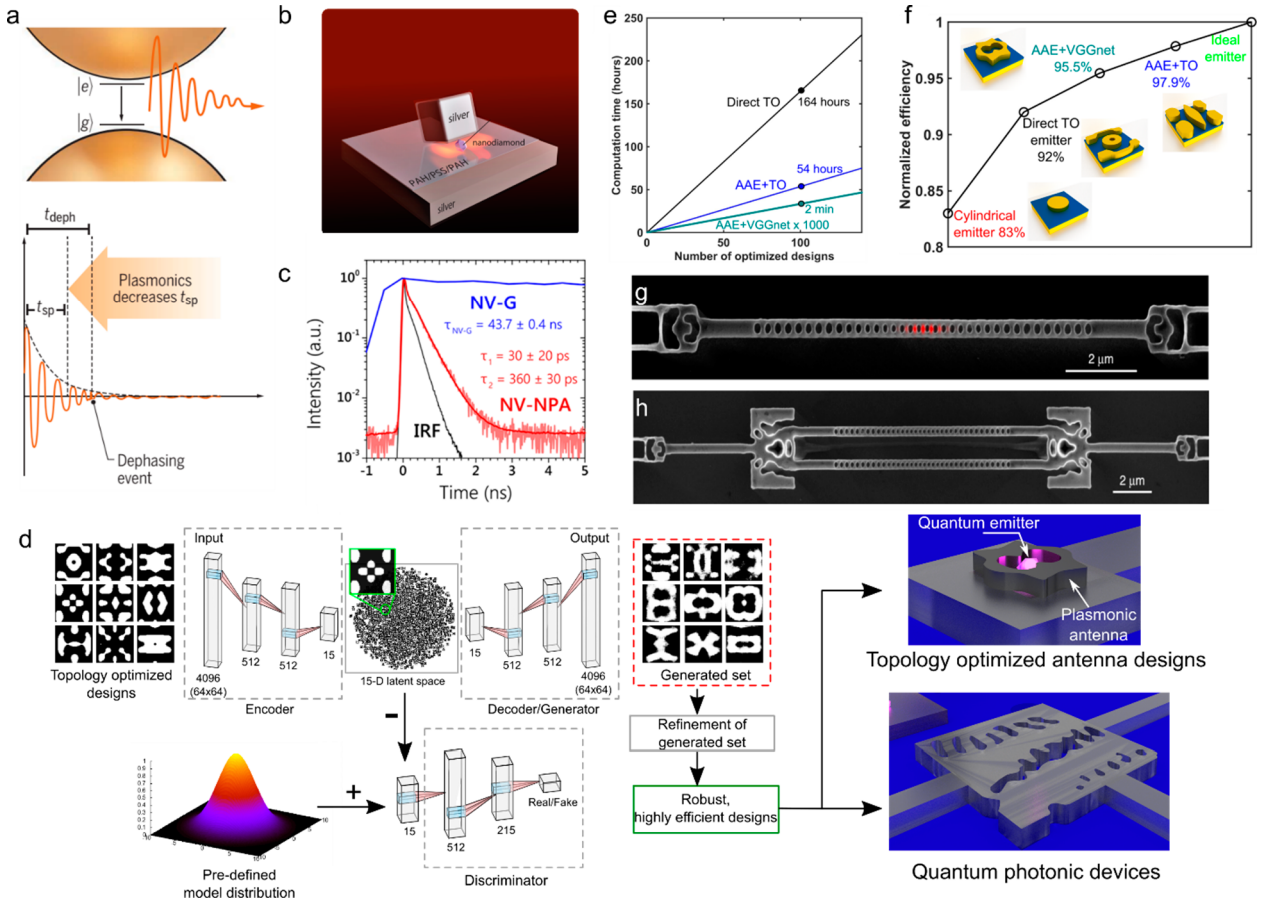

Figure 4. (a) Plasmonic speed-up.[53] The enhancement of the light−matter interaction in plasmonic cavities can shorten emitter's spontaneous emission time t_{sp} to beat the dephasing time t_{depth}. (b, c) Room-T, ultrafast quantum emitter.[54] (b) In an all-silver nanopatch antenna (NPA) structure, a silver nanocube is deposited on a silver substrate, with a nanodiamond, containing an NV center placed in between. (c) Fluorescence decay curves indicate nanodiamond on a coverslip glass substrate (NV-G) (blue), the NV coupled to a nanopatch antenna (NV-NPA) (red), and the instrument response function (IRF) (black). (d−f) AAE-assisted optimization framework.[66] For quantum device design optimization, the AAE network is trained on topology optimized designs. The encoder is mapping geometrical features into the compressed design space, while decoder/generator learns to generate design shapes based on the compressed space coordinates during the training phase. Discriminator forces encoder and decoder to form the compressed space with a predefined distribution. (e) Dependence of the computational time of the direct TO (black), AAE+TO-based optimization (blue), and AAE+VGGnet (cyan) on the number of the optimized high-efficiency resonant patterns. For the generation of 100s of designs, direct TO requires 164 h, the AAE+TO refinement approach needs 54 h, while the AAE+VGGnet approach requires only 2 min for the generation of highly efficient (>80%) 100 designs. The AAE+VGGnet-based approach is 1620× faster than the AAE+TO approach and more than 4900× faster than direct TO. (f) Comparison of the efficiencies of the obtained best designs for all used optimization methods within this work. The AAE optimization followed by additional TO refinement ensures the best solution and almost maximum possible result of the problem under consideration. While the AAE+VGGnet approach ensures tremendous speedup of the optimization search and relatively high overall device efficiency. Insets show the best antenna designs in the sets for different optimization frameworks. (g, h) Inverse design of diamond photonics.[111] SEM images of the optimized (g) photonic crystal cavity with inverse-designed vertical couplers placed on both ends of the structure and (h) diamond photonic circuit, which could be used to entangle two emitters inside the two cavities. The circuit consists of a grating coupler, followed by a waveguide-splitter, and two resonators, the outputs of which are then recombined in a waveguide-splitter and coupled off-chip through a grating coupler. (a) Adapted with permission from ref 53. Copyright 2019 AAAS. (b, c) Adapted with permission from ref 54. Copyright 2018 ACS. (d−f) Adapted with permission from ref 66. Copyright 2020 AIP Publishing. (g, h) Adapted with permission from ref 111. Copyright 2019 Nature Research.

different aspects of artificially engineered materials have been adapted for quantum applications. Plasmonics, or metal nano-optics, promises to bring new functionalities and interaction regimes to quantum photonics. In particular, nonlinearities at the single-photon level[43] and ultrabright single-photon emission[44,45] have been theoretically predicted. Recent experiments demonstrate that gap-plasmon nanoantennas are prime candidates for plasmon-enhanced single-photon emission.[46−51] Extremely tight mode confinement in single nm-size cavities can even lead to strong interaction with single dipoles at room temperature.[52] The challenge of utilizing plasmonic elements in quantum photonic integrated circuits is their high optical losses. It has recently been shown that it is possible to circumvent these losses by designing nanostructures where the outcoupling of light into a lossless dielectric environment happens at the same time scale or faster than the photon absorption[53] (Figure 4a). Incorporating plasmonic structures into quantum photonic systems offers both ultrafast operation speed (∼THz) and room temperature (room-T) performance. A record-high single-photon intensity from room-T single nitrogen-vacancy (NV) centers in diamond, at 35 million photons per second,[54] demonstrates the promise of on-

https://dx.doi.org/10.1021/acsphotonics.0c00960
ACS Photonics XXXX, XXX, XXX−XXX

demand single-photon production in plasmonic nanostructures (Figure 4b,c). Specifically, a nanopatch antenna, consisting of an all-crystalline-silver nanocube coupled with an NV center in a nanodiamond (Figure 4b), has been used for showcasing a two-orders of magnitude average fluorescence lifetime shortening and a ∼90-fold increase in the average detected saturated intensity of the quantum emission (Figure 4c).

In all of the cases of artificially engineered materials, the structural design plays a central role within the device development cycle. Incorporating advanced optimization techniques into the meta-device(nanoantennas, cavities, on-chip components) will significantly increase the efficiency and will open the way for the realization of highly multifunctional quantum photonic meta-structures (Figure 4d). Advanced optimization could, for example, be used to achieve deterministic control over the single-photon emission, such as the emission directionality and rate. This would require solving a multiconstrained problem by developing approaches that go well beyond conventional optimization techniques.

Conventionally, there are two major design development approaches (i) intuition-based, which relies on the prior knowledge and scientific intuition; (ii) advanced optimization frameworks, which solve inverse-design problems and lead to nonintuitive solutions. The first approach typically yields meta-structures with somewhat simplified geometrical shapes (e.g., spheres, cylinders, and core−shell particles) and, hence, limited performance. Such performance limitations are a consequence of the reduced number of available degrees of freedom in the optical response due to the simplistic topology of the device unit cell. The advanced optimization techniques ensure much higher efficiency due to the complex shape/topologies of the optimized structures.While evolutional and adjoint optimization methods have been widely used in photonics,[55−57] conventional frameworks are limited by the computational power requirement, which scales up with the increasing dimension of the parametric space. Recently, different ML algorithms have been proposed and applied to photonic and plasmonic problems.[58−61] Along with pure discriminative schemes, in which the DNNs are used to predict the parameters and optical response of nanoantenna designs with simplistic geometries, several hybrid approaches have been proposed.[62−65] Specifically, various generative networks (such as generative adversarial networks (GANs)[64] and autoencoders) have been coupled with a topology optimization framework and applied for nanophotonic design optimization. For example, integrating an adjoint topology optimization method with adversarial autoencoder (AAE), consisting of three neural networks (encoder, decoder, and discriminator) allows one to perform optimization of a device with complex topologies much faster than a conventional adjoint formalism[66] (Figure 4d). In particular, the authors coupled an AAE network with (i) topology optimization based refinement (AAE+TO) and (ii) pretrained VGGnet neural network for generated designs postselection process (AAE+VGGnet). The performance of the developed optimization frameworks was benchmarked by optimizing a thermally emitting metasurface for thermophotovoltaics. The comparison of the developed frameworks vs the conventional optimization approaches is shown in Figure 4e,f. Figure 4e shows the computational costs of direct topology optimization (black), AAE+TO refinement (blue), and AAE+VGGnet (red) approaches. Direct TO requires 164 h for the generation of 100 designs, the AAE +TO refinement approach needs 54 h, while the AAE +VGGnet approach requires only 2 min. Thus, the developed AAE+VGGnet approach ensures 1620× speed-up in comparison with the AAE+TO approach and it is more than 4900 times faster than direct TO. The efficiencies of best designs obtained by optimization of cylindrical design (simple topology), direct TO, AAE+VGGnet, and AAE+TO are shown in Figure 4f. The efficiencies are normalized to the fundamental limit of the TiN thermal emitter. The developed AAE frameworks ensure almost perfect performance with 98% (AAE+TO) and 96% (AAE+VGGnet) efficiency, while conventional frameworks ensure only 92% (direct TO) and 83% (simple design). Such a hybrid scheme opens up a possibility to perform a physics-driven global optimization scheme directly inside the compressed design space formed by the AAE.[67] Thus, the resulting optimization targets not only the complex topology of the antenna but also the best material composition as well as fabrication parameters. Hybrid ML-optimization approaches could provide the best-performing quantum photonic devices in terms of single-photon emission as well as compatibility with quantum photonic circuitry. Recently, the fundamental limits for the quantum emission enhancement in the plasmonic cavity-based SPEs have been studied.[68] It has been shown that by appropriately predesigning the cavity and antenna modes of the gap-plasmon based SPEs, it is possible to achieve quantum emission rates up to hundreds of THz and the far-field radiation efficiency close to unity. This analysis clearly shows that by applying advanced ML-assisted optimization to the cavity design optimization it is possible to substantially enhance the room-T quantum emission.

ML-assisted optimization could also enable on-demand entangled state generation utilizing spontaneous parametric down-conversion processes (SPDC) in nonlinear dielectric structures. Recently, AlGaAs nanoantennas have been used for the generation of the two-photon quantum states at telecommunication wavelengths.[69] Using the Mie resonances in nanocylindrical antennas, photon pairs were generated at a rate of 35 Hz. However, the efficiency of photon pair generation is low due to nonoptimal resonance mode coupling at the pump, idler, and signal frequencies. Here, ML-assisted topology optimization could lead to substantially increased emission rates by using more complex resonant mode coupling as well as coherent generation of multiphoton quantum states via multiplexing several antennas within one metasurface.

The proposed optimization techniques open the way for novel applications in free-space quantum communication and sensing protocols, and can also be applied to develop a family of highly efficient, multifunctional elements of quantum photonic circuits and on-chip structures (Figure 4d). Recently, it has been shown that topology optimization can be efficiently applied to the development of diamond-based quantum photonic circuits such as free-space couplers integrated with photonic crystal cavities and inverse-designed waveguide-splitters (Figure 4g,h).

Yet another important optimization challenge that can be addressed via ML assisted optimization frameworks is efficient, on-demand on-chip integration of quantum emitter. The realization of scalable quantum photonics demands deterministic and efficient on-chip integration of an array of quantum emitters via passive optical elements, such as cavities or couplers.[70,71] The choice of a suitable material platform is another important factor since commonly used silicon is optically lossy at shorter wavelength range (<1.1 μm), within

https://dx.doi.org/10.1021/acsphotonics.0c00960
ACS Photonics XXXX, XXX, XXX−XXX

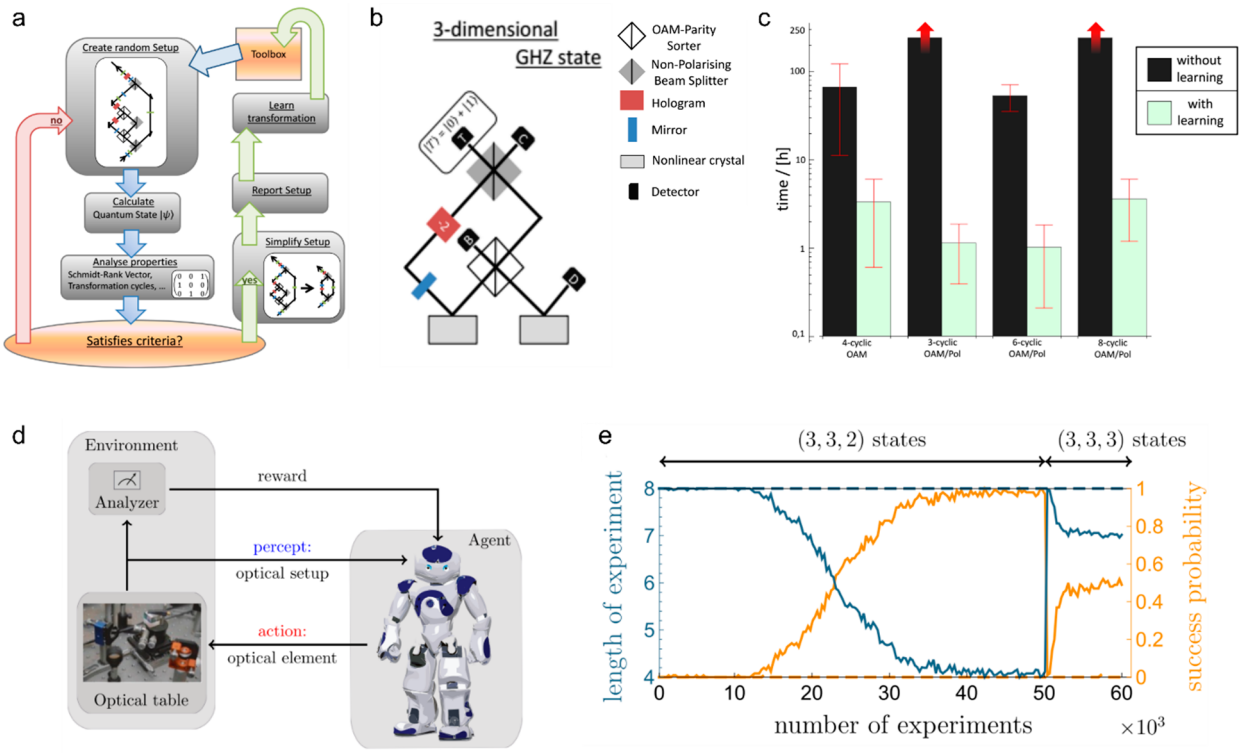

Figure 5. (a–c) Active learning for quantum experiment optimization.[100] (a) Working principle of the algorithm. The experiment is initiated via a random selection of the elements from a basic toolbox. After each iteration, the performance of the developed setup is assessed via calculating the quantum state and analyzing its properties. The efficiency of the performance is calculated through the comparison with the user defined criteria. If these criteria are not satisfied, the algorithm starts over again, otherwise. the experiment is simplified and reported, together with all relevant information for the user. (b) The experimental implementation for a 3-dimensional 3-partite GHZ-state. (c) Comparison of performance with and without the ability to learn (log-scale). Green shows the average time required in the case where the algorithm can learn useful transformations (the algorithm was executed 10 times with the same initial conditions). Black shows the time it requires without the ability to learn. The experiments for 3-cyclic and 8-cyclic transformations were not found (within 250 h) without learning, while experiments for 4-cyclic and 6-cyclic rotation were found three and four times in 250 h, respectively. (d, e) Reinforcement learning for novel quantum experiment designing.[26] (e) The reinforcement algorithm for quantum experiment development is realized via the agent placing the elements from the basic toolbox into the experimental table. The decision on the next iteration is decided via the rewarding agent if the figure of merit(difference between produced and goal quantum states' properties) met. (e) Results of learning new experiments. Average length of experiment and success probability in each of the 6×10^4 experiments. The maximal length of an experiment is $L = 8$. During the first 5×10^4 experiments an agent is rewarded for obtaining a (3, 3, 2) state, and during the last 10^4 experiments, the same agent is rewarded when finding a (3, 3, 3) state. The average success probability shows how probable it is for the PS agent to find a rewarded state in a given experiment. Solid/dashed lines show simulations of the PS agent that learns how to generate a (3, 3, 3) state from the beginning with/without prior learning of setups that produce a (3, 3, 2) state. (a–c) Adapted with permission from ref 100. Copyright 2016 American Physical Society. (d, e) Adapted with permission from ref 26. Copyright 2018 National Academy of Sciences.

which most of the single-photon sources are emitting. Recently, various on-chip coupling methods for single-photon sources have been proposed, including tapered optical fibers[72−75] in situ direct laser written[76] or electron beam lithographed,[77] diamond,[78−80] 2D material-based,[81−83] dielectric[84−91] or plasmonic structures.[92−94] Along with efficient coupling, the strong enhancement of the spontaneous emission of quantum emitters should be achieved by these coupling methods. Recently, it has been shown that a "quantum plasmonic launcher" which consists of nanodiamonds with single NV centers sandwiched between two epitaxial silver films, can dramatically decrease the lifetime of the NV center (~10 ps) and a couple more than half of the emission into in-plane propagating surface plasmon polaritons (SPPs).[95] The proposed architecture offers record-high fluorescence lifetime shortening (~7000×), which is higher than those obtained previously for dielectric-loaded waveguides,[93,94] the V-groove system,[96] and metal nanowires.[97] The plasmonic launcher could pave the way to on-chip integration of single-photon sources with extreme emission rates and THz operation rates. Further optimization would maximize the coupling efficiency while maintaining the high emission rate by providing optimal design that adiabatically converts the SPP waves into the fundamental mode of the waveguide.[98,99]

AUTOMATIZATION OF THE QUANTUM EXPERIMENTS

The true limits of the machines in the context of quantum photonics are much broader than advanced data postprocessing and lies in the domains of active and reinforcement learning. Recently, several efforts have been made in the field of designing complex experiments based on the autonomous learning models. The modern quantum mechanical experiments are used to probe the basic concepts of quantum theories. However, to be able to probe more sophisticated theoretical concepts, it is necessary to develop much more complex experimental machinery and measurement techniques. The designing of such complex experiments based on human perception and intuition might be a difficult task. Recently, it is demonstrated that active learning can be adapted

https://dx.doi.org/10.1021/acsphotonics.0c00960
ACS Photonics XXXX, XXX, XXX−XXX

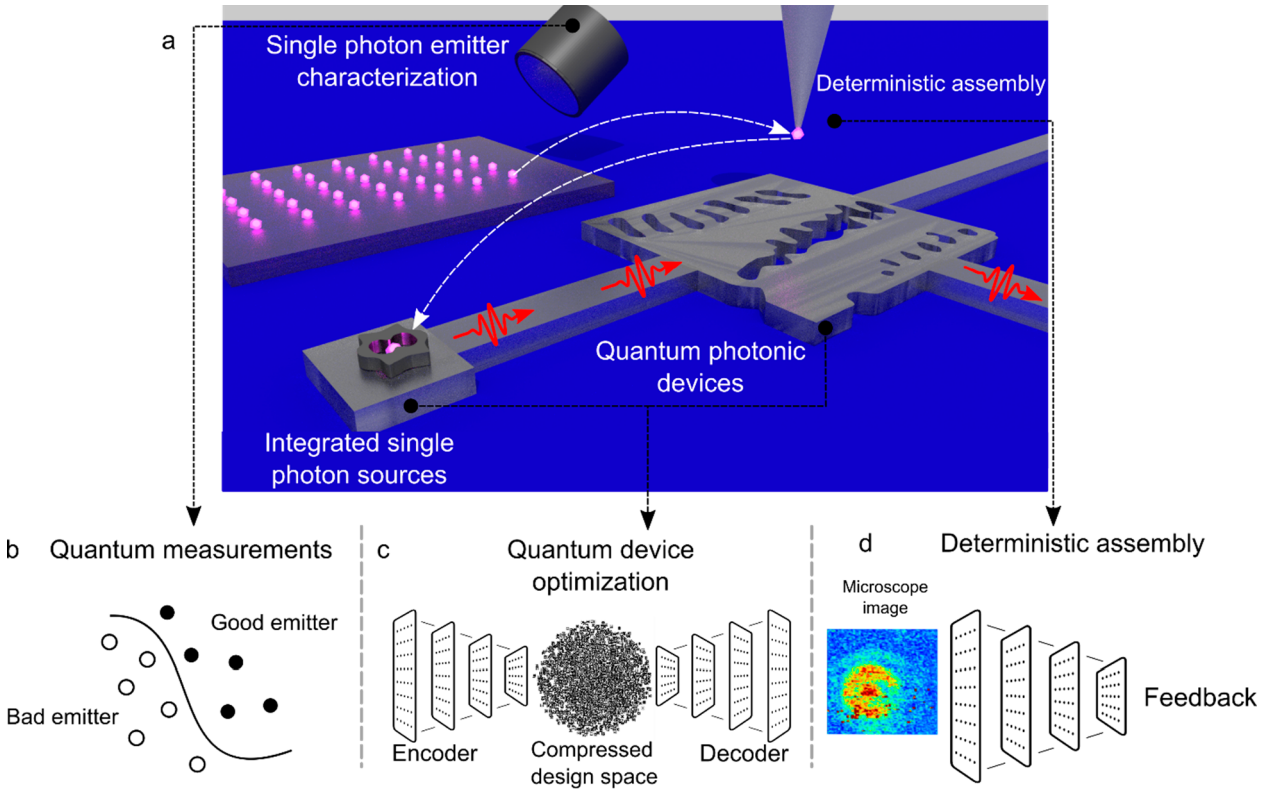

Figure 6. (a) Schematics of the ML-assisted quantum circuitry elements design and deterministic assembly. (b) "Good/bad" quantum emitter classification via ML-assisted rapid quantum measurements, where ML enables multiclass classification based on sparse data sets. (c) Quantum circuit elements are shape-optimized via generative network coupled with topology optimization. (d) CNN-assisted automatic driver enables the deterministic assembly of circuitry elements.

for the development of a quantum experiment with the goal of creation and manipulation of complex quantum states.[100] Within developed frameworks, the quantum phenomena as teleportation,[101,102] quantum interference,[103] quantum erasure,[104] and entanglement are considered as the main building block, and the algorithm has learned to find the best combination of them for achieving predefined quantum states. The general flow of the developed framework is shown in Figure 5a. The machine uses the optical elements from the toolbox and randomly assembles new experiment setups. The performance of the developed experimental setup is assessed at each iteration via calculation of the resulted quantum state, the transformation, and its properties. The algorithm stops upon meeting the user-defined criteria. During the search process, the machine can learn from the experience and can extend the basic toolbox by including information on the already developed experimental schemes. Such learning process leads to significantly speed-up in subsequent discoveries. Developed framework has been used for (1) realization of high-dimensional multipartite entanglement, so-called the Greenberger-Horne-Zeilinger (GHZ) state, and (2) realization of high-dimensional cyclic rotations of quantum states. Within example 1, the algorithm has been able to find 51 experiments in ∼150 h, which can be used for the realization of the quantum states that are entangled differently, including the first experimentally realizable scheme of a high-dimensional GHZ state (Figure 5b). Notably, the developed experimental schemes contain interesting novel "tricks", which are counter-intuitive for human perception. For example, one of the four paths that come directly from the nonlinear crystals has not been mixed with any other arm (arm D in Figure 5b). Such asymmetry in the experimental scheme is the result of the fact that for double SPDC events the two photon pairs may come from the same crystal. Leaving one path unmixed leads to the erasure of such double-pair emission events in 4-fold coincidence detection. Within example 2, authors have applied a developed framework to the realization of high-dimensional cyclic rotations, which are special cases of high-dimensional unitary transformations of quantum states. Such transformations are necessary for the realization of a novel, high-dimensional quantum information protocols,[38,39] as well as in the creation of high-dimensional Bell-states. The basic toolbox for such problems has been set to polarizing and nonpolarizing beam splitters, dove prisms, mirrors, holograms, and halfwave plates. Within this showcase example, authors have demonstrated the advantages of the algorithm with the learning of the novel toolbox elements versus the approach without such ability. The quantities comparison of the required time for different cases of the cyclic operations is shown in Figure 5c. Specifically, it has been demonstrated that an approach without the learning procedure requires up to 250 h of search for identification of only 3 and 4 experimental schemes for 4-cyclic and 6-cyclic rotations, while such an approach failed to find any experimental schemes for 3-cyclic and an 8-cyclic rotation. For the case of an algorithm with learning ability, it required <3.5 h to find experimental realization for all of the cyclic rotation experiments. As a result of the developed machine-driven framework, several of these experimental proposals have been implemented successfully in the laboratory[105−107] and have led to the discovery of new quantum techniques.[108,109]

Along with an active learning algorithm, reinforcement learning has been applied for the development of quantum

https://dx.doi.org/10.1021/acsphotonics.0c00960
ACS Photonics XXXX, XXX, XXX−XXX

experiments.[26] It has been demonstrated that the developed approach can be used not only for complex experimental schemes development but also ensures the discovery of nontrivial experimental techniques. The scheme of the developed ML algorithm is shown in Figure 5d. As in the previous approach, the agent has an access to a set of optical elements (toolbox), with which it generates experiments: It sequentially places the chosen elements on the (simulated) table; following the placement of an element, the quantum state generated by the corresponding setup, i.e., configuration of optical elements, is analyzed. Depending on the state estimation the agent receives a reward. Then the agent proceeds with another iteration by placing additional elements into the table. Due to the different sources of noise, which resulted due to imperfection in the alignment of the optical elements, the total number of elements in the experiment is limited to a finite number. Along with the efficient experimental scheme discovery, the agent can extend the basic toolbox by the learning process and its memory. Such knowledge helps him to perform more efficient experiment scheme reconstruction. Within this work, the authors consider two types of problems: (i) minimization of the elements of the existing experiments and (ii) development of novel experimental schemes. The first example targeted the development of the experimental scheme for the creation of a quantum state with (3,3,2) Schmidt−Rank vector (SRV). To emphasize the importance of the learning process, the same agent has been used for the development of the experiment for (3,3,3) SRV quantum state generation. Here authors probed whether the agent can leverage on the acquired knowledge during the first part of the reinforcement learning process and develop a more complex experimental setup efficiently. Figure 5e shows the main result of the first example. The agent has been able to minimize the number of used elements to 4 (the smallest number of the elements for (3,3,2) SRV case) within 3×10^4 experiments. After the 5×10^4 experiments, the agent has been rewarded for the (3,3,3) SRV state generation. As a result, the experimental schemes with the smallest possible length of the experiment have been obtained within additional $\sim 3 \times 10^3$ runs. This clearly shows the agent can leverage on the acquired knowledge during the previous optimization runs.

DISCUSSION AND CONCLUSION

ML-assisted quantum photonics is an emerging field that offers a great potential for transforming the field of integrated quantum photonics. Various machine and deep learning techniques have been adapted for several important quantum photonics problems, including efficient data postprocessing, which allowed for a significant speed-up of quantum optical measurements and the development of novel quantum experiments for the realization of complex quantum states based on the reinforcement learning. While the first demonstrations of ML-assisted quantum measurement speed-ups and efficient device design are very encouraging, the fundamental limits of ML techniques and artificial intelligence, in general, are yet to be explored. We envision that ML-assisted quantum photonics will become crucial for the realization of scalable integrated quantum circuits, for example, choosing the right SPEs for the task, design of efficient photonic devices, deterministic assembly of the quantum circuit elements, and conducting resource-optimized data analysis. Figure 6a represents the authors' vision for machine-driven techniques in the field of quantum photonics. ML techniques have already demonstrated their efficiency in predicting the quality of the quantum emission based on sparse autocorrelation data. We believe that ML algorithms can be adapted to perform similar predictions for several key properties of quantum emitters at once (quantum purity, lifetime, stability, and indistinguishability) based on extremely sparse measurements, which will significantly speed-up the quantum emitter characterization and preselection process (Figure 6b). As shown above, the advanced optimization techniques can be significantly enhanced via coupling with generative networks. ML-assisted optimization could play a critical role in the development of quantum circuits elements, such as efficient couplers and on-chip devices for efficient quantum states transduction and transformations (Figure 6c). Neural networks can also enable a key step in realizing large-scale quantum photonic systems, namely, in enabling the deterministic assembly of quantum sources and quantum devices with the nanometer scale precision (Figure 6d). Recently, it has been shown that an atomic force microscope (AFM) tip can be used for the deterministic assembly of plasmonic nanopatch antennas (e.g., plasmonic cubes coupled to nanodiamonds) with gap sizes below 20 nm.[110] While the current techniques typically require manual manipulation, the coupling of the AFM-based deterministic assembly with a pretrained CNN can uniquely enable rapid, automated nanoassembly via all-neural-network-driven AFM machinery (Figure 6d). The CNN can also be trained to take the AFM scan data or a microscope image as an input and return the displacement vector needed to operate (move, pick or place nanoparticle), as an output, such that it can be used to automatically drive the AFM tip. This approach will open up entirely new ways for the realization of automated, large-scale, precise, and rapid deterministic nano-assembly of quantum sources as well as other on-chip quantum devices.

We highlighted several promising directions for ML-assisted quantum photonics that can be adapted for many other quantum applications. ML-assisted rapid characterization of quantum emitters could lead to the large-scale integrated quantum circuits prototyping by speeding up conventional measurement techniques and offering novel measurement frameworks. Also, ML-assisted nanodevice optimization techniques might be adapted to solve the inverse-problems of quantum device design to develop new types of plasmonic-assisted SPEs or SPDC based sources of complex entangled photonic states. Moreover, rapid CNN-based data processing can help to realize high-precision deterministic assembly of quantum circuitry elements.

AUTHOR INFORMATION

Corresponding Author

Alexandra Boltasseva − *School of Electrical and Computer Engineering, Birck Nanotechnology Center and Purdue Quantum Science and Engineering Institute, Purdue University, West Lafayette, Indiana 47906, United States; The Quantum Science Center (QSC), a National Quantum Information Science Research Center of the U.S. Department of Energy (DOE), Oak Ridge, Tennessee 37931, United States;* orcid.org/0000-0001-8905-2605; Email: aeb@purdue.edu

Authors

Zhaxylyk A. Kudyshev − *School of Electrical and Computer Engineering, Birck Nanotechnology Center and Purdue*

https://dx.doi.org/10.1021/acsphotonics.0c00960
ACS Photonics XXXX, XXX, XXX−XXX

Quantum Science and Engineering Institute, Purdue University, West Lafayette, Indiana 47906, United States; The Quantum Science Center (QSC), a National Quantum Information Science Research Center of the U.S. Department of Energy (DOE), Oak Ridge, Tennessee 37931, United States; orcid.org/0000-0002-6955-0890

Vladimir M. Shalaev − *School of Electrical and Computer Engineering, Birck Nanotechnology Center and Purdue Quantum Science and Engineering Institute, Purdue University, West Lafayette, Indiana 47906, United States; The Quantum Science Center (QSC), a National Quantum Information Science Research Center of the U.S. Department of Energy (DOE), Oak Ridge, Tennessee 37931, United States*

Complete contact information is available at: https://pubs.acs.org/10.1021/acsphotonics.0c00960

Notes

The authors declare no competing financial interest.

■ ACKNOWLEDGMENTS

This work is supported by the U.S. Department of Energy (DOE), Office of Science through the Quantum Science Center (QSC), a National Quantum Information Science Research Center and National Science Foundation Award 2015025-ECCS.

■ REFERENCES

(1) Aspuru-Guzik, A.; Walther, P. Photonic Quantum Simulators. *Nat. Phys.* **2012**, *8* (4), 285−291.
(2) Tang, H.; Lin, X.-F.; Feng, Z.; Chen, J.-Y.; Gao, J.; Sun, K.; Wang, C.-Y.; Lai, P.-C.; Xu, X.-Y.; Wang, Y.; et al. Experimental Two-Dimensional Quantum Walk on a Photonic Chip. *Sci. Adv.* **2018**, *4* (5), eaat3174.
(3) Blatt, R.; Wineland, D. Entangled States of Trapped Atomic Ions. *Nature* **2008**, *453* (7198), 1008−1015.
(4) Bloch, I. Quantum Coherence and Entanglement with Ultracold Atoms in Optical Lattices. *Nature* **2008**, *453* (7198), 1016−1022.
(5) Clarke, J.; Wilhelm, F. K. Superconducting Quantum Bits. *Nature* **2008**, *453* (7198), 1031−1042.
(6) Hanson, R.; Kouwenhoven, L. P.; Petta, J. R.; Tarucha, S.; Vandersypen, L. M. K. Spins in Few-Electron Quantum Dots. *Rev. Mod. Phys.* **2007**, *79* (4), 1217−1265.
(7) Aharonovich, I.; Englund, D.; Toth, M. Solid-State Single-Photon Emitters. *Nat. Photonics* **2016**, *10* (10), 631−641.
(8) O'Brien, J. L.; Furusawa, A.; Vučković, J. Photonic Quantum Technologies. *Nat. Photonics* **2009**, *3* (12), 687−695.
(9) Krizhevsky, A.; Sutskever, I.; Hinton, G. E. ImageNet Classification with Deep Convolutional Neural Networks. *Commun. ACM* **2017**, *60*, 84−90.
(10) Cho, K.; van Merrienboer, B.; Gulcehre, C.; Bahdanau, D.; Bougares, F.; Schwenk, H.; Bengio, Y. Learning Phrase Representations Using RNN Encoder−Decoder for Statistical Machine Translation. In *Proceedings of the 2014 Conference on Empirical Methods in Natural Language Processing (EMNLP)*; Association for Computational Linguistics: Stroudsburg, PA, U.S.A., 2014; pp 1724−1734.
(11) Hinton, G.; Deng, L.; Yu, D.; Dahl, G.; Mohamed, A.; Jaitly, N.; Senior, A.; Vanhoucke, V.; Nguyen, P.; Sainath, T.; et al. Deep Neural Networks for Acoustic Modeling in Speech Recognition: The Shared Views of Four Research Groups. *IEEE Signal Process. Mag.* **2012**, *29* (6), 82−97.
(12) Sanchez-Lengeling, B.; Aspuru-Guzik, A. Inverse Molecular Design Using Machine Learning: Generative Models for Matter Engineering. *Science* **2018**, *361* (6400), 360−365.
(13) Goh, G. B.; Hodas, N. O.; Vishnu, A. Deep Learning for Computational Chemistry. *J. Comput. Chem.* **2017**, *38* (16), 1291−1307.
(14) Zahavy, T.; Dikopoltsev, A.; Moss, D.; Haham, G. I.; Cohen, O.; Mannor, S.; Segev, M. Deep Learning Reconstruction of Ultrashort Pulses. *Optica* **2018**, *5* (5), 666.
(15) Rivenson, Y.; Göröcs, Z.; Günaydin, H.; Zhang, Y.; Wang, H.; Ozcan, A. Deep Learning Microscopy. *Optica* **2017**, *4* (11), 1437.
(16) van Esbroeck, N. M.; Lennon, D. T.; Moon, H.; Nguyen, V.; Vigneau, F.; Camenzind, L. C.; Yu, L.; Zumbühl, D. M.; Briggs, G. A. D.; Sejdinovic, D.; et al. Quantum Device Fine-Tuning Using Unsupervised Embedding Learning. *New J. Phys.* **2020**, *22* (9), 095003.
(17) Moon, H.; Lennon, D. T.; Kirkpatrick, J.; van Esbroeck, N. M.; Camenzind, L. C.; Yu, L.; Vigneau, F.; Zumbühl, D. M.; Briggs, G. A. D.; Osborne, M. A.; et al. Machine Learning Enables Completely Automatic Tuning of a Quantum Device Faster than Human Experts. *Nat. Commun.* **2020**, *11* (1), 4161.
(18) Lennon, D. T.; Moon, H.; Camenzind, L. C.; Yu, L.; Zumbühl, D. M.; Briggs, G. A. D.; Osborne, M. A.; Laird, E. A.; Ares, N. Efficiently Measuring a Quantum Device Using Machine Learning. *npj Quantum Inf.* **2019**, *5* (1), 79.
(19) Altman, N. S. An Introduction to Kernel and Nearest-Neighbor Nonparametric Regression. *Am. Stat.* **1992**, *46* (3), 175−185.
(20) Ho, T. K. The Random Subspace Method for Constructing Decision Forests. *IEEE Trans. Pattern Anal. Mach. Intell.* **1998**, *20* (8), 832−844.
(21) Hsu, C.-W.; Lin, C.-J. A Comparison of Methods for Multiclass Support Vector Machines. *IEEE Trans. Neural Networks* **2002**, *13* (2), 415−425.
(22) Shalev-Shwartz, S.; Ben-David, S. *Understanding Machine Learning*; Cambridge University Press: Cambridge, 2014.
(23) Tolles, J.; Meurer, W. J. Logistic Regression. *JAMA* **2016**, *316* (5), 533.
(24) Ghahramani, Z. Probabilistic Machine Learning and Artificial Intelligence. *Nature* **2015**, *521* (7553), 452−459.
(25) Dunjko, V.; Briegel, H. J. Machine Learning & Artificial Intelligence in the Quantum Domain: A Review of Recent Progress. *Rep. Prog. Phys.* **2018**, *81* (7), 074001.
(26) Melnikov, A. A.; Poulsen Nautrup, H.; Krenn, M.; Dunjko, V.; Tiersch, M.; Zeilinger, A.; Briegel, H. J. Active Learning Machine Learns to Create New Quantum Experiments. *Proc. Natl. Acad. Sci. U. S. A.* **2018**, *115* (6), 1221−1226.
(27) Cong, I.; Choi, S.; Lukin, M. D. Quantum Convolutional Neural Networks. *Nat. Phys.* **2019**, *15* (12), 1273−1278.
(28) Torlai, G.; Timar, B.; van Nieuwenburg, E. P. L.; Levine, H.; Omran, A.; Keesling, A.; Bernien, H.; Greiner, M.; Vuletić, V.; Lukin, M. D.; Melko, R. G.; Endres, M. Integrating Neural Networks with a Quantum Simulator for State Reconstruction. *Phys. Rev. Lett.* **2019**, *123* (23), 230504.
(29) Palmieri, A. M.; Kovlakov, E.; Bianchi, F.; Yudin, D.; Straupe, S.; Biamonte, J. D.; Kulik, S. Experimental Neural Network Enhanced Quantum Tomography. *npj Quantum Inf.* **2020**, *6* (1), 20.
(30) You, C.; Quiroz-Juarez, M. A.; Lambert, A.; Bhusal, N.; Dong, C.; Perez-Leija, A.; Javaid, A.; Leon-Montiel, R. d. J.; Magana-Loaiza, O. S. Identification of Light Sources Using Machine Learning. *Appl. Phys. Rev.* **2020**, *7* (2), 021404.
(31) Santagati, R.; Gentile, A. A.; Knauer, S.; Schmitt, S.; Paesani, S.; Granade, C.; Wiebe, N.; Osterkamp, C.; McGuinness, L. P.; Wang, J.; et al. Magnetic-Field Learning Using a Single Electronic Spin in Diamond with One-Photon Readout at Room Temperature. *Phys. Rev. X* **2019**, *9* (2), 021019.
(32) Wiebe, N.; Granade, C.; Ferrie, C.; Cory, D. G. Hamiltonian Learning and Certification Using Quantum Resources. *Phys. Rev. Lett.* **2014**, *112* (19), 190501.
(33) Hentschel, A.; Sanders, B. C. Machine Learning for Precise Quantum Measurement. *Phys. Rev. Lett.* **2010**, *104* (6), 063603.

(34) Naruse, M.; Berthel, M.; Drezet, A.; Huant, S.; Aono, M.; Hori, H.; Kim, S.-J. Single-Photon Decision Maker. *Sci. Rep.* **2015**, *5* (1), 13253.
(35) Kudyshev, Z. A.; Bogdanov, S. I.; Isacsson, T.; Kildishev, A. V.; Boltasseva, A.; Shalaev, V. M. Rapid Classification of Quantum Sources Enabled by Machine Learning. *Adv. Quantum Technol.* **2020**, *3* (10), 2000067.
(36) Gatto Monticone, D.; Katamadze, K.; Traina, P.; Moreva, E.; Forneris, J.; Ruo-Berchera, I.; Olivero, P.; Degiovanni, I. P.; Brida, G.; Genovese, M. Beating the Abbe Diffraction Limit in Confocal Microscopy via Nonclassical Photon Statistics. *Phys. Rev. Lett.* **2014**, *113* (14), 143602.
(37) Tenne, R.; Rossman, U.; Rephael, B.; Israel, Y.; Krupinski-Ptaszek, A.; Lapkiewicz, R.; Silberberg, Y.; Oron, D. Super-Resolution Enhancement by Quantum Image Scanning Microscopy. *Nat. Photonics* **2019**, *13* (2), 116−122.
(38) Rossman, U.; Tenne, R.; Solomon, O.; Kaplan-Ashiri, I.; Dadosh, T.; Eldar, Y. C.; Oron, D. Rapid Quantum Image Scanning Microscopy by Joint Sparse Reconstruction. *Optica* **2019**, *6* (10), 1290.
(39) Joannopoulos, J. D.; Villeneuve, P. R.; Fan, S. Photonic Crystals: Putting a New Twist on Light. *Nature* **1997**, *386*, 143−149.
(40) Shalaev, V. M. Optical Negative-Index Metamaterials. *Nat. Photonics* **2007**, *1* (1), 41−48.
(41) Song, M.; Kudyshev, Z. A.; Yu, H.; Boltasseva, A.; Shalaev, V. M.; Kildishev, A. V. Achieving Full-Color Generation with Polarization-Tunable Perfect Light Absorption. *Opt. Mater. Express* **2019**, *9* (2), 779.
(42) Kildishev, A. V.; Boltasseva, A.; Shalaev, V. M. Planar Photonics with Metasurfaces. *Science* **2013**, *339*, 1232009.
(43) Gullans, M.; Chang, D. E.; Koppens, F. H. L.; de Abajo, F. J. G.; Lukin, M. D. Single-Photon Nonlinear Optics with Graphene Plasmons. *Phys. Rev. Lett.* **2013**, *111* (24), 247401.
(44) Bozhevolnyi, S. I.; Khurgin, J. B. Fundamental Limitations in Spontaneous Emission Rate of Single-Photon Sources. *Optica* **2016**, *3* (12), 1418.
(45) Tame, M. S.; McEnery, K. R.; Özdemir, Ş. K.; Lee, J.; Maier, S. A.; Kim, M. S. Quantum Plasmonics. *Nat. Phys.* **2013**, *9* (6), 329−340.
(46) Yang, J.; Faggiani, R.; Lalanne, P. Light Emission in Nanogaps: Overcoming Quenching. *Nanoscale Horizons* **2016**, *1* (1), 11−13.
(47) Kongsuwan, N.; Demetriadou, A.; Chikkaraddy, R.; Benz, F.; Turek, V. A.; Keyser, U. F.; Baumberg, J. J.; Hess, O. Suppressed Quenching and Strong-Coupling of Purcell-Enhanced Single-Molecule Emission in Plasmonic Nanocavities. *ACS Photonics* **2018**, *5* (1), 186−191.
(48) Faggiani, R.; Yang, J.; Lalanne, P. Quenching, Plasmonic, and Radiative Decays in Nanogap Emitting Devices. *ACS Photonics* **2015**, *2* (12), 1739−1744.
(49) Chikkaraddy, R.; de Nijs, B.; Benz, F.; Barrow, S. J.; Scherman, O. A.; Rosta, E.; Demetriadou, A.; Fox, P.; Hess, O.; Baumberg, J. J. Single-Molecule Strong Coupling at Room Temperature in Plasmonic Nanocavities. *Nature* **2016**, *535* (7610), 127−130.
(50) Akselrod, G. M.; Argyropoulos, C.; Hoang, T. B.; Ciracì, C.; Fang, C.; Huang, J.; Smith, D. R.; Mikkelsen, M. H. Probing the Mechanisms of Large Purcell Enhancement in Plasmonic Nanoantennas. *Nat. Photonics* **2014**, *8* (11), 835−840.
(51) Hoang, T. B.; Akselrod, G. M.; Argyropoulos, C.; Huang, J.; Smith, D. R.; Mikkelsen, M. H. Ultrafast Spontaneous Emission Source Using Plasmonic Nanoantennas. *Nat. Commun.* **2015**, *6* (1), 7788.
(52) Ojambati, O. S.; Chikkaraddy, R.; Deacon, W. D.; Horton, M.; Kos, D.; Turek, V. A.; Keyser, U. F.; Baumberg, J. J. Quantum Electrodynamics at Room Temperature Coupling a Single Vibrating Molecule with a Plasmonic Nanocavity. *Nat. Commun.* **2019**, *10* (1), 1049.
(53) Bogdanov, S. I.; Boltasseva, A.; Shalaev, V. M. Overcoming Quantum Decoherence with Plasmonics. *Science* **2019**, *364* (6440), 532−533.
(54) Bogdanov, S. I.; Shalaginov, M. Y.; Lagutchev, A. S.; Chiang, C. C.; Shah, D.; Baburin, A. S.; Ryzhikov, I. A.; Rodionov, I. A.; Kildishev, A. V.; Boltasseva, A.; et al. Ultrabright Room-Temperature Sub-Nanosecond Emission from Single Nitrogen-Vacancy Centers Coupled to Nanopatch Antennas. *Nano Lett.* **2018**, *18* (8), 4837−4844.
(55) Wang, F.; Jensen, J. S.; Sigmund, O. Robust Topology Optimization of Photonic Crystal Waveguides with Tailored Dispersion Properties. *J. Opt. Soc. Am. B* **2011**, *28* (3), 387.
(56) Molesky, S.; Lin, Z.; Piggott, A. Y.; Jin, W.; Vucković, J.; Rodriguez, A. W. Inverse Design in Nanophotonics. *Nat. Photonics* **2018**, *12* (11), 659−670.
(57) Oskooi, A.; Mutapcic, A.; Noda, S.; Joannopoulos, J. D.; Boyd, S. P.; Johnson, S. G. Robust Optimization of Adiabatic Tapers for Coupling to Slow-Light Photonic-Crystal Waveguides. *Opt. Express* **2012**, *20* (19), 21558.
(58) Shen, Y.; Harris, N. C.; Skirlo, S.; Prabhu, M.; Baehr-Jones, T.; Hochberg, M.; Sun, X.; Zhao, S.; Larochelle, H.; Englund, D.; et al. Deep Learning with Coherent Nanophotonic Circuits. *Nat. Photonics* **2017**, *11* (7), 441−446.
(59) Ma, W.; Cheng, F.; Liu, Y. Deep-Learning-Enabled On-Demand Design of Chiral Metamaterials. *ACS Nano* **2018**, *12* (6), 6326−6334.
(60) Malkiel, I.; Mrejen, M.; Nagler, A.; Arieli, U.; Wolf, L.; Suchowski, H. Plasmonic Nanostructure Design and Characterization via Deep Learning. *Light: Sci. Appl.* **2018**, *7* (1), 60.
(61) Ma, W.; Liu, Z.; Kudyshev, Z. A.; Boltasseva, A.; Cai, W.; Liu, Y. Deep Learning for the Design of Photonic Structures. *Nat. Photonics* **2020**, DOI: 10.1038/s41566-020-0685-y.
(62) Ma, W.; Cheng, F.; Xu, Y.; Wen, Q.; Liu, Y. Probabilistic Representation and Inverse Design of Metamaterials Based on a Deep Generative Model with Semi-Supervised Learning Strategy. *Adv. Mater.* **2019**, *31* (35), 1901111.
(63) Liu, Z.; Zhu, D.; Rodrigues, S. P.; Lee, K. T.; Cai, W. Generative Model for the Inverse Design of Metasurfaces. *Nano Lett.* **2018**, *18* (10), 6570−6576.
(64) Jiang, J.; Sell, D.; Hoyer, S.; Hickey, J.; Yang, J.; Fan, J. A. Free-Form Diffractive Metagrating Design Based on Generative Adversarial Networks. *ACS Nano* **2019**, *13* (8), 8872−8878.
(65) Jiang, J.; Fan, J. A. Global Optimization of Dielectric Metasurfaces Using a Physics-Driven Neural Network. *Nano Lett.* **2019**, *19* (8), 5366−5372.
(66) Kudyshev, Z. A.; Kildishev, A. V.; Shalaev, V. M.; Boltasseva, A. Machine-Learning-Assisted Metasurface Design for High-Efficiency Thermal Emitter Optimization. *Appl. Phys. Rev.* **2020**, *7* (2), 021407.
(67) Kudyshev, Z. A.; Kildishev, A. V.; Shalaev, V. M.; Boltasseva, A. Machine Learning Assisted Global Optimization of Photonic Devices. *Nanophotonics* **2020**, *10*, 371.
(68) Bogdanov, S. I.; Makarova, O. A.; Xu, X.; Martin, Z. O.; Lagutchev, A. S.; Olinde, M.; Shah, D.; Chowdhury, S. N.; Gabidullin, A. R.; Ryzhikov, I. A.; et al. Ultrafast Quantum Photonics Enabled by Coupling Plasmonic Nanocavities to Strongly Radiative Antennas. *Optica* **2020**, *7* (5), 463.
(69) Marino, G.; Solntsev, A. S.; Xu, L.; Gili, V. F.; Carletti, L.; Poddubny, A. N.; Rahmani, M.; Smirnova, D. A.; Chen, H.; Lemaître, A.; et al. Spontaneous Photon-Pair Generation from a Dielectric Nanoantenna. *Optica* **2019**, *6* (11), 1416.
(70) Kimble, H. J. The Quantum Internet. *Nature* **2008**, *453* (7198), 1023−1030.
(71) Benson, O. Assembly of Hybrid Photonic Architectures from Nanophotonic Constituents. *Nature* **2011**, *480* (7376), 193−199.
(72) Schröder, T.; Fujiwara, M.; Noda, T.; Zhao, H.-Q.; Benson, O.; Takeuchi, S. A Nanodiamond-Tapered Fiber System with High Single-Mode Coupling Efficiency. *Opt. Express* **2012**, *20* (10), 10490.
(73) Liebermeister, L.; Petersen, F.; Münchow, A. V.; Burchardt, D.; Hermelbracht, J.; Tashima, T.; Schell, A. W.; Benson, O.; Meinhardt, T.; Krueger, A.; et al. Tapered Fiber Coupling of Single Photons Emitted by a Deterministically Positioned Single Nitrogen Vacancy Center. *Appl. Phys. Lett.* **2014**, *104* (3), 031101.

https://dx.doi.org/10.1021/acsphotonics.0c00960
ACS Photonics XXXX, XXX, XXX−XXX

(74) Fujiwara, M.; Yoshida, K.; Noda, T.; Takashima, H.; Schell, A. W.; Mizuochi, N.; Takeuchi, S. Manipulation of Single Nanodiamonds to Ultrathin Fiber-Taper Nanofibers and Control of NV-Spin States toward Fiber-Integrated λ -Systems. *Nanotechnology* **2016**, *27* (45), 455202.
(75) Patel, R. N.; Schröder, T.; Wan, N.; Li, L.; Mouradian, S. L.; Chen, E. H.; Englund, D. R. Efficient Photon Coupling from a Diamond Nitrogen Vacancy Center by Integration with Silica Fiber. *Light: Sci. Appl.* **2016**, *5* (2), e16032−e16032.
(76) Shi, Q.; Sontheimer, B.; Nikolay, N.; Schell, A. W.; Fischer, J.; Naber, A.; Benson, O.; Wegener, M. Wiring up Pre-Characterized Single-Photon Emitters by Laser Lithography. *Sci. Rep.* **2016**, *6* (1), 31135.
(77) Schnauber, P.; Schall, J.; Bounouar, S.; Höhne, T.; Park, S.-I.; Ryu, G.-H.; Heindel, T.; Burger, S.; Song, J.-D.; Rodt, S.; et al. Deterministic Integration of Quantum Dots into On-Chip Multimode Interference Beamsplitters Using in Situ Electron Beam Lithography. *Nano Lett.* **2018**, *18* (4), 2336−2342.
(78) Faraon, A.; Barclay, P. E.; Santori, C.; Fu, K.-M. C.; Beausoleil, R. G. Resonant Enhancement of the Zero-Phonon Emission from a Colour Centre in a Diamond Cavity. *Nat. Photonics* **2011**, *5* (5), 301−305.
(79) Burek, M. J.; Meuwly, C.; Evans, R. E.; Bhaskar, M. K.; Sipahigil, A.; Meesala, S.; Machielse, B.; Sukachev, D. D.; Nguyen, C. T.; Pacheco, J. L.; et al. Fiber-Coupled Diamond Quantum Nanophotonic Interface. *Phys. Rev. Appl.* **2017**, *8* (2), 024026.
(80) Bhaskar, M. K.; Sukachev, D. D.; Sipahigil, A.; Evans, R. E.; Burek, M. J.; Nguyen, C. T.; Rogers, L. J.; Siyushev, P.; Metsch, M. H.; Park, H.; et al. Quantum Nonlinear Optics with a Germanium-Vacancy Color Center in a Nanoscale Diamond Waveguide. *Phys. Rev. Lett.* **2017**, *118* (22), 223603.
(81) Schell, A. W.; Takashima, H.; Tran, T. T.; Aharonovich, I.; Takeuchi, S. Coupling Quantum Emitters in 2D Materials with Tapered Fibers. *ACS Photonics* **2017**, *4* (4), 761−767.
(82) Fröch, J. E.; Kim, S.; Mendelson, N.; Kianinia, M.; Toth, M.; Aharonovich, I. Coupling Hexagonal Boron Nitride Quantum Emitters to Photonic Crystal Cavities. *ACS Nano* **2020**, *14* (6), 7085.
(83) Kim, S.; Duong, N. M. H.; Nguyen, M.; Lu, T.; Kianinia, M.; Mendelson, N.; Solntsev, A.; Bradac, C.; Englund, D. R.; Aharonovich, I. Integrated on Chip Platform with Quantum Emitters in Layered Materials. *Adv. Opt. Mater.* **2019**, *7* (23), 1901132.
(84) Gschrey, M.; Gericke, F.; Schüßler, A.; Schmidt, R.; Schulze, J.-H.; Heindel, T.; Rodt, S.; Strittmatter, A.; Reitzenstein, S. In Situ Electron-Beam Lithography of Deterministic Single-Quantum-Dot Mesa-Structures Using Low-Temperature Cathodoluminescence Spectroscopy. *Appl. Phys. Lett.* **2013**, *102* (25), 251113.
(85) Zadeh, I. E.; Elshaari, A. W.; Jöns, K. D.; Fognini, A.; Dalacu, D.; Poole, P. J.; Reimer, M. E.; Zwiller, V. Deterministic Integration of Single Photon Sources in Silicon Based Photonic Circuits. *Nano Lett.* **2016**, *16* (4), 2289−2294.
(86) Gould, M.; Schmidgall, E. R.; Dadgostar, S.; Hatami, F.; Fu, K.-M. C. Efficient Extraction of Zero-Phonon-Line Photons from Single Nitrogen-Vacancy Centers in an Integrated GaP-on-Diamond Platform. *Phys. Rev. Appl.* **2016**, *6* (1), 011001.
(87) Kim, J.-H.; Aghaeimeibodi, S.; Richardson, C. J. K.; Leavitt, R. P.; Englund, D.; Waks, E. Hybrid Integration of Solid-State Quantum Emitters on a Silicon Photonic Chip. *Nano Lett.* **2017**, *17* (12), 7394−7400.
(88) Tonndorf, P.; Del Pozo-Zamudio, O.; Gruhler, N.; Kern, J.; Schmidt, R.; Dmitriev, A. I.; Bakhtinov, A. P.; Tartakovskii, A. I.; Pernice, W.; Michaelis de Vasconcellos, S.; et al. On-Chip Waveguide Coupling of a Layered Semiconductor Single-Photon Source. *Nano Lett.* **2017**, *17* (9), 5446−5451.
(89) Mouradian, S. L.; Schroder, T.; Poitras, C. B.; Li, L.; Goldstein, J.; Chen, E. H.; Walsh, M.; Cardenas, J.; Markham, M. L.; Twitchen, D. J.; Lipson, M.; Englund, D.; et al. Scalable Integration of Long-Lived Quantum Memories into a Photonic Circuit. *Phys. Rev. X* **2015**, *5* (3), 031009.
(90) Davanco, M.; Liu, J.; Sapienza, L.; Zhang, C.-Z.; De Miranda Cardoso, J. V.; Verma, V.; Mirin, R.; Nam, S. W.; Liu, L.; Srinivasan, K. Heterogeneous Integration for On-Chip Quantum Photonic Circuits with Single Quantum Dot Devices. *Nat. Commun.* **2017**, *8* (1), 889.
(91) Böhm, F.; Nikolay, N.; Pyrlik, C.; Schlegel, J.; Thies, A.; Wicht, A.; Tränkle, G.; Benson, O. On-Chip Integration of Single Solid-State Quantum Emitters with a SiO 2 Photonic Platform. *New J. Phys.* **2019**, *21* (4), 045007.
(92) Kewes, G.; Schoengen, M.; Neitzke, O.; Lombardi, P.; Schönfeld, R.-S.; Mazzamuto, G.; Schell, A. W.; Probst, J.; Wolters, J.; Löchel, B.; et al. A Realistic Fabrication and Design Concept for Quantum Gates Based on Single Emitters Integrated in Plasmonic-Dielectric Waveguide Structures. *Sci. Rep.* **2016**, *6* (1), 28877.
(93) Siampour, H.; Kumar, S.; Bozhevolnyi, S. I. Nanofabrication of Plasmonic Circuits Containing Single Photon Sources. *ACS Photonics* **2017**, *4* (8), 1879−1884.
(94) Siampour, H.; Kumar, S.; Davydov, V. A.; Kulikova, L. F.; Agafonov, V. N.; Bozhevolnyi, S. I. On-Chip Excitation of Single Germanium Vacancies in Nanodiamonds Embedded in Plasmonic Waveguides. *Light: Sci. Appl.* **2018**, *7* (1), 61.
(95) Chiang, C.-C.; Bogdanov, S. I.; Makarova, O. A.; Xu, X.; Saha, S.; Shah, D.; Wang, D.; Lagutchev, A. S.; Kildishev, A. V.; Boltasseva, A.; et al. Chip-Compatible Quantum Plasmonic Launcher. *Adv. Opt. Mater.* **2020**, *8*, 2000889.
(96) Bermúdez-Ureña, E.; Gonzalez-Ballestero, C.; Geiselmann, M.; Marty, R.; Radko, I. P.; Holmgaard, T.; Alaverdyan, Y.; Moreno, E.; García-Vidal, F. J.; Bozhevolnyi, S. I.; et al. Coupling of Individual Quantum Emitters to Channel Plasmons. *Nat. Commun.* **2015**, *6* (1), 7883.
(97) Akimov, A. V.; Mukherjee, A.; Yu, C. L.; Chang, D. E.; Zibrov, A. S.; Hemmer, P. R.; Park, H.; Lukin, M. D. Generation of Single Optical Plasmons in Metallic Nanowires Coupled to Quantum Dots. *Nature* **2007**, *450* (7168), 402−406.
(98) Briggs, R. M.; Grandidier, J.; Burgos, S. P.; Feigenbaum, E.; Atwater, H. A. Efficient Coupling between Dielectric-Loaded Plasmonic and Silicon Photonic Waveguides. *Nano Lett.* **2010**, *10* (12), 4851−4857.
(99) Khurgin, J. B.; Sun, G. Practicality of Compensating the Loss in the Plasmonic Waveguides Using Semiconductor Gain Medium. *Appl. Phys. Lett.* **2012**, *100* (1), 011105.
(100) Krenn, M.; Malik, M.; Fickler, R.; Lapkiewicz, R.; Zeilinger, A. Automated Search for New Quantum Experiments. *Phys. Rev. Lett.* **2016**, *116* (9), 090405.
(101) Bennett, C. H.; Brassard, G.; Crépeau, C.; Jozsa, R.; Peres, A.; Wootters, W. K. Teleporting an Unknown Quantum State via Dual Classical and Einstein-Podolsky-Rosen Channels. *Phys. Rev. Lett.* **1993**, *70* (13), 1895−1899.
(102) Wang, X.-L.; Cai, X.-D.; Su, Z.-E.; Chen, M.-C.; Wu, D.; Li, L.; Liu, N.-L.; Lu, C.-Y.; Pan, J.-W. Quantum Teleportation of Multiple Degrees of Freedom of a Single Photon. *Nature* **2015**, *518* (7540), 516−519.
(103) Hong, C. K.; Ou, Z. Y.; Mandel, L. Measurement of Subpicosecond Time Intervals between Two Photons by Interference. *Phys. Rev. Lett.* **1987**, *59* (18), 2044−2046.
(104) Scully, M. O.; Drühl, K. Quantum Eraser: A Proposed Photon Correlation Experiment Concerning Observation and "Delayed Choice" in Quantum Mechanics. *Phys. Rev. A: At., Mol., Opt. Phys.* **1982**, *25* (4), 2208−2213.
(105) Malik, M.; Erhard, M.; Huber, M.; Krenn, M.; Fickler, R.; Zeilinger, A. Multi-Photon Entanglement in High Dimensions. *Nat. Photonics* **2016**, *10* (4), 248−252.
(106) Schlederer, F.; Krenn, M.; Fickler, R.; Malik, M.; Zeilinger, A. Cyclic Transformation of Orbital Angular Momentum Modes. *New J. Phys.* **2016**, *18* (4), 043019.
(107) Babazadeh, A.; Erhard, M.; Wang, F.; Malik, M.; Nouroozi, R.; Krenn, M.; Zeilinger, A. High-Dimensional Single-Photon Quantum Gates: Concepts and Experiments. *Phys. Rev. Lett.* **2017**, *119* (18), 180510.

https://dx.doi.org/10.1021/acsphotonics.0c00960
ACS Photonics XXXX, XXX, XXX−XXX

(108) Krenn, M.; Hochrainer, A.; Lahiri, M.; Zeilinger, A. Entanglement by Path Identity. *Phys. Rev. Lett.* **2017**, *118* (8), 080401.
(109) Krenn, M.; Gu, X.; Zeilinger, A. Quantum Experiments and Graphs: Multiparty States as Coherent Superpositions of Perfect Matchings. *Phys. Rev. Lett.* **2017**, *119* (24), 240403.
(110) Bogdanov, S. I.; Makarova, O. A.; Lagutchev, A. S.; Shah, D.; Chiang, C.-C.; Saha, S.; Baburin, A. S.; Ryzhikov, I. A.; Rodionov, I. A.; Kildishev, A. V. Deterministic Integration of Single Nitrogen-Vacancy Centers into Nanopatch Antennas. *arXiv:1902.05996 [quant-ph]* **2019**, na.
(111) Dory, C.; Vercruysse, D.; Yang, K. Y.; Sapra, N. V.; Rugar, A. E.; Sun, S.; Lukin, D. M.; Piggott, A. Y.; Zhang, J. L.; Radulaski, M.; et al. Inverse-Designed Diamond Photonics. *Nat. Commun.* **2019**, *10* (1), 3309.

https://dx.doi.org/10.1021/acsphotonics.0c00960
ACS Photonics XXXX, XXX, XXX−XXX